Direct Measurement of Auger Electrons Emitted from a Semiconductor Light-Emitting Diode under Electrical Injection: Identification of the Dominant Mechanism for Efficiency Droop

Justin Iveland,[1] Lucio Martinelli,[2] Jacques Peretti,[2] James S. Speck,[1] and Claude Weisbuch[1,2,*]

[1] *Materials Department, University of California, Santa Barbara, California 93106, USA*

[2] *Laboratoire de Physique de la Matière Condensée, CNRS-Ecole Polytechnique, 91128 Palaiseau Cedex, France*

(Received 25 December 2012; published 25 April 2013)

We report on the unambiguous detection of Auger electrons by electron emission spectroscopy from a cesiated InGaN/GaN light-emitting diode under electrical injection. Electron emission spectra were measured as a function of the current injected in the device. The appearance of high energy electron peaks simultaneously with an observed drop in electroluminescence efficiency shows that hot carriers are being generated in the active region (InGaN quantum wells) by an Auger process. A linear correlation was measured between the high energy emitted electron current and the "droop current"—the missing component of the injected current for light emission. We conclude that the droop phenomenon in GaN light-emitting diodes originates from the excitation of Auger processes.

DOI: 10.1103/PhysRevLett.110.177406 PACS numbers: 85.60.Jb, 73.40.Kp, 79.20.Fv, 85.35.Be

The Auger carrier recombination mechanism is universal in semiconductors and plays a major role in limiting the performance of devices such as long wavelength telecommunications lasers [1] or, with a more limited role, solar cells under high excitation [2]. The most prevalent mechanism is a three-particle interaction, two electrons and one hole, or two holes and one electron, in which an electron-hole pair recombines releasing its energy nonradiatively by promoting the remaining particle into a higher energy state.

In GaN light-emitting diodes (LEDs), Auger recombination is also invoked as a possible origin of the so-called efficiency droop phenomenon, i.e., the drop in light emission quantum efficiency at high carrier injection [3]. However, the interpretation of the droop phenomenon remains highly controversial, in spite of its importance and many studies on it. Many proposed mechanisms rely on the enhanced nonradiative (NR) recombination at point defects in either quantum barriers or surrounding majority carrier regions when carriers are no longer localized in the high radiative recombination efficiency regions of quantum wells (QWs): carrier overflow from the QWs into regions of efficient NR recombination [4–6], loss of current injection efficiency [5], density-activated defect recombination [7], insufficient hole injection efficiency leading to electron leakage [8]. Auger recombination in the QWs is, however, a somewhat favored mechanism [3], with possibly an early onset induced by the reduction in active volume due to current crowding [9] or by carrier localization [10,11]. Up to now, the evidence of this process comes from analysis of carrier dynamics [3], either continuous wave or by time-resolved measurements where the n^2p or np^2 dependence of the recombination rate is observed (n and p are the electron and hole concentrations, respectively). Additional support for Auger recombination comes from the fact that compensation processes for the Auger recombination seem to offer diminished droop, thus enabling operation at higher current densities, such as using thicker active regions that reduce carrier densities [12]. However, the remedies do not yield unambiguous identification of the droop origin, as several mechanisms can be impacted by a given change in LED design—for instance reducing carrier concentration could also diminish carrier leakage [8].

There is so far no direct evidence of Auger carriers in semiconductors by observing the remaining higher energy particle. Such direct observation requires a spectroscopic measurement of hot electrons. Spectroscopy of low energy electrons emitted into vacuum is a classical method to study hot electrons in semiconductors. Already in 1967, Eden *et al.* [13] measured hot electron emission spectra under excitation with visible light. Since that time, this technique has been widely used to study the electronic structure [14] and hot electron transport properties [15,16] of various semiconductors and junctions. Multivalley transport toward the surface was observed due to efficient transfer to long-lived side conduction valleys. This phenomenon was also recently evidenced in nitrides [17,18].

In this Letter we report on the direct measurement of Auger electrons generated by carrier recombination in semiconductors by electron emission spectroscopy. The experiments were performed on GaN-based LEDs. Energy analysis of electrons emitted from the device into vacuum is performed as a function of forward-bias current. The signature of Auger electrons is observed through high energy peaks which appear in the electron energy distribution curves (EDCs) at high injected current densities. The Auger electron current is found to correlate with the simultaneously observed droop in emission efficiency.

The principle of our experiment is shown in Fig. 1(a). Electrons and holes are injected in the active layers (InGaN QWs) of a LED. The p-type GaN surface is activated by

 © 2013 American Physical Society

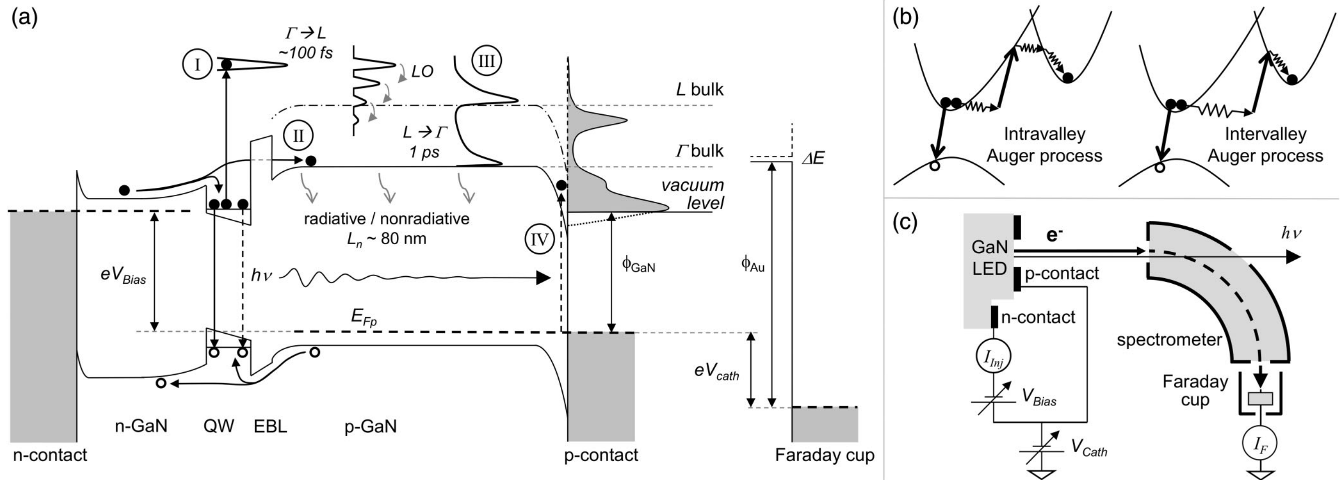

FIG. 1. (a) Energy levels for a biased LED structure emitting electrons in vacuum. (b) Schematics of hot electron generation into the L valley by an *eeh* Auger process: Left, the Auger electron is created in the Γ band (intravalley process) and transferred to the L valley; right, the Auger electron is created in the L valley (intervalley process). (c) Schematics of the electron energy analysis setup.

cesium deposition to negative electron affinity (NEA) where the minimum of the conduction band (CB) in bulk p-type GaN lies above the vacuum level at the surface. Electrons reaching the surface are emitted into vacuum where their energy distribution is measured. During the transport, different processes give rise to different contributions in the emitted electron spectrum.

Let us first discuss thermalized electron emission. Cold electrons can be injected in the p side at low energy by either bypassing capture into the QWs or by overflowing the QWs and subsequently overcoming the electron barrier layer (EBL), by tunneling or by thermionic emission [process II in Fig. 1(a)]. These "overshoot" electrons that reach the surface (a significant fraction will be lost by recombination in the 200 nm thick p region) will largely be thermalized, even those electrons launched in the p side over the EBL. Indeed, the LO-phonon emission time is 9 fs in GaN [19], which and is much shorter than the ~1 ps transit time for electrons with thermal velocity of a few 10^5 m/s. Photoemission excited by the LED light, below the GaN band gap [20], reabsorbed near the surface [process IV in Fig. 1(a)] either due to impurity band transitions or to Franz-Keldysh transitions, could also generate low energy electron emission.

Highly energetic electrons can be created by Auger recombination in the QWs through an electron-electron-hole process (*eeh*) which launches electrons with an initial energy equal to the recombining e-h pair in the QW, ~2.7 eV in the blue [process I in Fig. 1(a)]. The Auger process can be direct, or mediated through a phonon or by disorder [Fig. 1(b)]. Theoretical calculations are still controversial [21,22]. As a result, Auger electrons may populate different valleys of the CB [process III in Fig. 1(a)]. If such electrons do not fully thermalize in the Γ CB before reaching the p-type GaN surface, observation of hot electrons is expected in the EDC.

In the present study the sample was a GaN-based LED structure from Walsin Lihwa (Taiwan), grown by metal-organic chemical vapor deposition on a flat (0001) sapphire substrate. It consists of a several μm thick undoped buffer layer, followed by a Si-doped n-type buffer, an 8 period $In_{0.18}Ga_{0.82}N/GaN$ multiple QW (3 nm thick InGaN QWs and 10 nm thick GaN barriers) a 40 nm thick $Al_{0.15}Ga_{0.85}N$ EBL, and a top 200 nm Mg-doped p layer ([Mg] approximately 1.8×10^{20} cm^{-3}). The n-side terminal is a Ti/Pt electrode. The sample has a p-side square Pt electrode (side 500 μm) with an array of 27 × 27 holes of 10 μm diameter holes to expose the p-type GaN.

The p-type GaN surface was prepared in NEA. The sample was first treated in an HCl-isopropanol solution [20] and then introduced in a UHV setup designed for low energy electron spectroscopy [16]. After annealing at 260 °C for ~30 min, the p-type GaN surface was cesiated. The surface activation by cesium deposition was optimized by monitoring the electron emission current. NEA was achieved without oxygen exposure. The work function ϕ_{GaN} was 2.3 eV and remained stable for several days. Electrons emitted from the junction were energy analyzed [Fig. 1(c)] with a resolution of 50 meV in a 90° electrostatic cylindrical deflection selector [14]. The spectrometer was set in the constant path energy mode and the spectrum was obtained by scanning the sample potential (p-contact potential) V_{cath}. In this operation mode, the selected electrons are those that may enter with zero kinetic energy in a grounded gold surface (Faraday cup) of work function $\phi_{Au} \sim 4.8$ eV. Their kinetic energy at emission is then: $E_k = \phi_{Au}\text{-}\phi_{GaN}\text{-}eV_{cath}$. The device was biased by applying a potential $V_{bias} + V_{cath}$ to the n-type GaN contact. For high current density measurements, pulsed current injection was used with a 5% duty cycle. We checked that the collected current was proportional to the duty cycle.

The overall collection and transmission efficiency of the spectrometer and electron optics is $\sim 10^{-3}$. All EDCs were corrected by multiplication by the ratio of the total emitted current to the integrated measured current at the Au Faraday cup. We have normalized the energy level of the LED structure at the QW position by subtracting the Ohmic drop in the n and p regions from the applied bias voltage as determined from the I-V characteristics.

Figure 2 shows the electroemission spectra measured at room temperature for different injected current. The noisy appearance of electron emission peaks at high injected current has two origins. First, the pulsed current injection with a 5% duty cycle reduces the time averaged emitted current by a factor of 20. Second, blurring of the emitted electron beam occurs, due to the stray electric fields from the n and p electrodes, which strongly diminishes the collection efficiency in the electron optics. This results in a reduction of the effective collected current intensity. The EDCs normalization procedure described above does correct this signal reduction but it cannot increase signal-to-noise ratio.

The electron energy is referred to the vacuum level at the p-type GaN emitting surface which is 2.3 eV above the Fermi level. As usual, if we assume that the surface band bending region (BBR) amplitude is large enough so that the CB minimum at the p-type GaN surface is below the vacuum level, the low energy onset of the emitted electron spectrum lies at the vacuum level position [14].

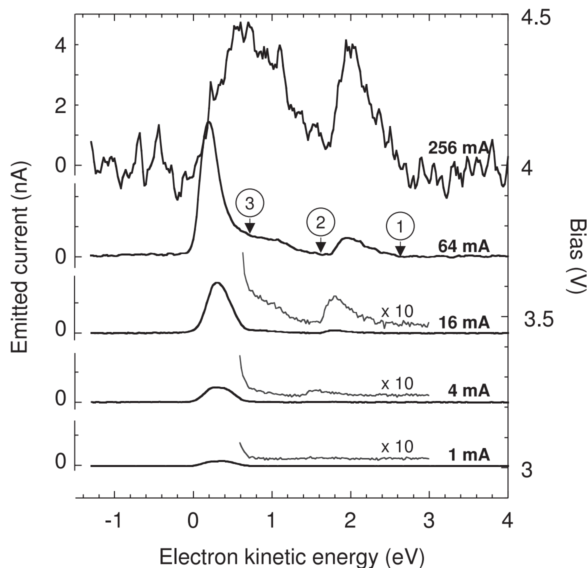

FIG. 2. Energy distribution curves for different injection currents. The baseline of each spectrum was shifted by the LED bias potential for that current (right-hand scale). Electron energy is referred to the vacuum level. When increasing injected current, high energy peaks appear around 2 eV signaling generation of hot carriers. The high energy thresholds of the different contributions to the energy distribution curves are labeled 1, 2, and 3 in the 64 mA spectrum.

At current below 1 mA (current density below 0.4 A/cm^2), a single low energy emission peak was observed and corresponds to thermalized electrons, either injected into the p side of the device junction, which were thermalized in the CB and subsequently underwent some further thermalization in the BBR or to photoemission excited by the LED light in the BBR. Because of the presence of an electron blocking layer, it is more probable that this low energy peak is due to LED light-excited photoemission from the BBR. This interpretation is supported by the observation of a similar photoemission peak (not shown here) under external excitation at energy close to the LED emission.

Higher energy peaks appeared at 4 mA injected current and higher. The main peak was ~ 1.5 eV above the low energy peak. A somewhat weaker intermediate peak was also observed at 0.3–0.4 eV above the low energy peak. The relative intensities of these two high energy peaks remain in the same ratio with increasing current, thus proving their common origin. The high energy threshold of the highest energy peak lies about 1.1 eV above the minimum of the CB in the bulk p-type GaN region [23].

The only viable mechanism to generate high energy carriers in the structure is Auger recombination. The bias potential dropped in the LED junction is close to the flat band potential and cannot produce hot electron injection. The other ways to generate hot carriers would be hot carrier launching by an energy barrier or by carrier heating by high electric fields. The former mechanism requires a barrier with an energy discontinuity that does not exist in the LED. The latter mechanism requires a region in the biased LED with a very high electric field but no such region exists in the LED, with the exception of the BBR. However, acceleration in the BBR electric field cannot promote electrons at higher total energy. Indeed, although electrons may gain kinetic energy in the BBR, their total energy at the surface remains smaller than in the bulk.

The available data on hot carriers in GaN support this interpretation of the high energy peak as due to another CB valley (for simplicity called here L). Transport measurements point to such a band, with quite some scatter about its energy position (see, e.g., Ref. [24]). Given the fast LO-phonon emission in GaN, it is not possible to directly observe Auger electrons at their initial kinetic energy after traversing 200 nm of p-type GaN. Actually, the phonon-assisted Auger process may directly yield Auger electrons within the L band [Fig. 1(b), right]. From their initial high energy in that band, electrons would thermalize quickly to its bottom: we expect phonon relaxation to be extremely fast in that band due to the high density of states and the many-valley states. In InP, for instance, intraside-valley phonon scattering is ~ 4 times faster than in the Γ valley [16]. Hence, the bottom of the L valley acts as a source of thermalized electrons for emission into the vacuum, as was observed in GaAs [13], InP [14], Si [15] and AlN [18].

This source emits an electron peak which high energy onset lies at the bottom of the L band in the bulk p-type GaN (kT is not observable in our setup). As the L valley minimum follows the BBR potential, electrons moving towards the surface relax part of their energy and the peak broadens towards lower energies when traversing the BBR. If the Auger process would occur in the Γ valley [Fig. 1(b)], electrons would also transfer in the L valley before reaching the surface as the time transfer from the Γ to L valley is very fast, at most 170 fs [25] as observed on the transfer threshold from the Γ valley. The experiment so far does not distinguish between the two Auger mechanisms.

The intermediate band, 300 meV above the lower peak, connected to the L valley emission, can originate from electrons scattered out of the L valley into the Γ band near the surface and thermalized at the bottom of the p-type GaN CB.

Analyzing the details of the results, the high energy features shift in energy with changing bias (Fig. 3). This shift is due to the rectifying character of the p-type GaN contact which drops most of the bias once flat band potential is reached in the p-n junction [26]. Thus, the positions of bulk p-type GaN bands (in particular of the L valley) relative to the constant p-contact potential (i.e., to the vacuum level) increases when increasing the bias from 3 to 4 V.

Electron emission in vacuum from forward-biased GaN p-n junctions was previously observed by Shaw *et al.* [27] with currents up to 5 A/cm^2. No new high energy peak was observed there as the carrier density, distributed over the carrier diffusion length, typically 100 nm, is quite smaller than in our 3 nm thick InGaN QWs.

Simultaneously with the measurement of the electroemission current and spectrum, we measured the light intensity emitted by the LED [Fig. 4(a)]. The "Auger electron current" (integrated high energy peak current) correlates with the droop current component as deduced from the dependence of optical power on current [Fig. 4(b)]. We consider the droop current as the supplementary current [labeled SC in Fig. 4(a)] necessary to obtain a given light output power [empty circles in Fig. 4(a)] when compared to that expected from a linear extrapolation [full line in Fig. 4(a)] from low to high currents.

The electron emission experiments presented here strongly support the observation of Auger electrons. However, a question remains: is it the dominant droop mechanism? Two pieces of evidence convince us that it is the case. First, if another mechanism were responsible for the droop, its effect would set in at lower current than Auger-electron generation. The concurrent appearance of the Auger-electron emission and the onset of droop shows that the Auger electron is indeed the major cause for droop. Second, the electron current emitted in vacuum has the right order of magnitude to account for the SC: we measure [Fig. 4(b)] a total electron emission current of 80 nA for a SC in the LED of 100 mA, thus an efficiency of $\sim 10^{-6}$. We can evaluate an efficiency in that range. First, most of the current is injected below the p electrode, and, therefore, does not yield any outside current due to the emission masking by the electrode. Only the fraction of injected current within a current spreading length from the edge of the unmasked apertures contributes to electron emission. For a 200 nm current spreading length, only 1% at most of injected current participates in emission. Second, only a fraction of the unmasked Auger electrons can be observed: half of them are emitted in the direction opposite to the surface; some of the Auger electrons transferred to the L valley do not reach the surface as they undergo the reverse transfer to the Γ valley (scattering time from L to Γ is 1 ps [25]), and a significant fraction recombine in the 200 nm p layer. The GaN emission quantum yield is in the $\sim 10^{-3}$ range as the cesiation was not optimized and used for a

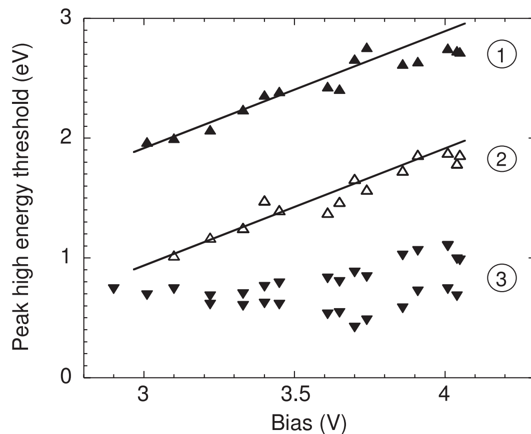

FIG. 3. Energy position of the three peak thresholds (labels 1, 2, and 3 in Fig. 2) under changing bias. As shown by the straight lines with slope 1, the hot electron energy increases with the applied bias due to a voltage drop at the p contact.

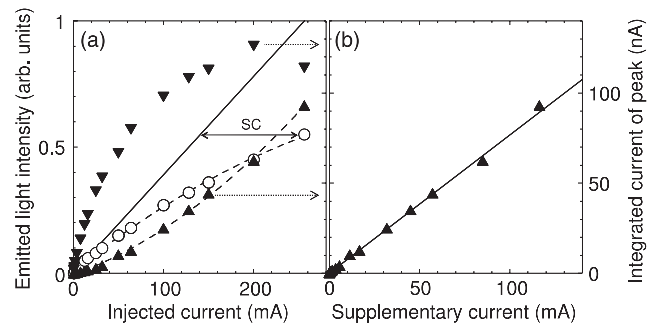

FIG. 4. (a) Integrated current of low (filled downward triangles) and high (filled upward triangles) energy peaks, and of the optical power (open circles) vs the injected current. The straight line is the expected optical output power in the absence of droop, extrapolated from low currents. (b) Integrated current of the high energy peak as a function of the supplementary current (SC, see text).

number of days. Another cause for a reduction in observed current is the recapture of electrons by the p electrode before they are attracted by the spectrometer entrance slit.

In conclusion, we have directly observed for the first time the generation of Auger electrons under electrical carrier injection in a semiconductor by the energy analysis of electrons emitted in vacuum from a p-n junction. In the studied structure, an InGaN LED, the measurement unambiguously assigns the droop in quantum efficiency observed at high injection current densities to Auger recombination of carriers and therefore brings essential information to a long-standing controversy.

The samples were kindly provided by H. T. Chen, K. M. Chen, and S.-C. Huang from Walsin Lihwa (Taiwan). The authors thank Y. Lassailly for fruitful discussions. The work at UCSB is supported by the Center for Energy Efficient Materials (CEEM), an Energy Frontier Research Center funded by the U. S. Department of Energy, Office of Science, Office of Basic Energy Sciences under Award No. DE-SC0001009.

*weisbuch@engineering.ucsb.edu

[1] See, e.g., A. Sugimura, IEEE J. Quantum Electron. **18**, 352 (1982).
[2] W. Shockley and H. J. Queisser, J. Appl. Phys. **32**, 510 (1961).
[3] Y. C. Shen, G. O. Müller, S. Watanabe, N. F. Gardner, A. Munkholm, and M. R. Krames, Appl. Phys. Lett. **91**, 141101 (2007).
[4] H. Zhao, G. Liu, R. A. Arif, and N. Tansu, Solid State Electron. **54**, 1119 (2010).
[5] L. Wang, C. Lu, J. Lu, L. Liu, N. Liu, Y. Chen, Y. Zhang, E. Gu, and X. Hu, Opt. Express **19**, 14 182 (2011).
[6] S. Hammersley, D. Watson-Parris, P. Dawson, M. J. Godfrey, T. J. Badcock, M. J. Kappers, C. McAleese, R. A. Oliver, and C. J. Humphreys, J. Appl. Phys. **111**, 083512 (2012).
[7] J. Hader, J. V. Moloney, and S. W. Koch, Appl. Phys. Lett. **96**, 221106 (2010).
[8] J. Xu *et al.*, Appl. Phys. Lett. **94**, 011113 (2009).
[9] Y. Y. Kudryk, A. K. Tkachenko, and A. V. Zinovchuk, Semicond. Sci. Technol. **27**, 055013 (2012).
[10] H.-Y. Ryu, D.-S. Shin, and J.-I. Shim, Appl. Phys. Lett. **100**, 131109 (2012).
[11] Y.-R. Wu, R. Shivaraman, K.-C. Wang, and J. S. Speck, Appl. Phys. Lett. **101**, 083505 (2012).
[12] N. F. Gardner, G. O. Müller, Y. C. Shen, G. Chen, S. Watanabe, W. Götz, and M. R. Krames, Appl. Phys. Lett. **91**, 243506 (2007).
[13] R. C. Eden, J. L. Moll, and W. E. Spicer, Phys. Rev. Lett. **18**, 597 (1967).
[14] H.-J. Drouhin, C. Hermann, and G. Lampel, Phys. Rev. B **31**, 3859 (1985); Y. Lassailly, P. Chiaradia, C. Hermann, and G. Lampel, *ibid.* **41**, 1266 (1990); J. Peretti, H.-J. Drouhin, D. Paget, and A. Mircea, *ibid.* **44**, 7999 (1991).
[15] I. Shahriary, J. R. Schwank, and F. G. Allen, J. Appl. Phys. **50**, 1428 (1979).
[16] J. Peretti, H.-J. Drouhin, and D. Paget, Phys. Rev. Lett. **64**, 1682 (1990).
[17] Z. Liu, F. Machuca, P. Pianetta, W. E. Spicer, and R. F. W. Pease, Appl. Phys. Lett. **85**, 1541 (2004).
[18] R. Collazo, R. Schlesser, A. Roskowski, P. Miraglia, R. F. Davis, and Z. Sitar, J. Appl. Phys. **93**, 2765 (2003).
[19] K. Wang, J. Simon, N. Goel, and D. Jena, Appl. Phys. Lett. **88**, 022103 (2006).
[20] O. E. Tereshchenko, G. É. Shaibler, A. S. Yaroshevich, S. V. Shevelev, A. S. Terekhov, V. V. Lundin, E. E. Zavarin, and A. I. Besyul'kin, Phys. Solid State **46**, 1949 (2004).
[21] E. Kioupakis, P. Rinke, K. T. Delaney, and C. G. Van de Walle, Appl. Phys. Lett. **98**, 161107 (2011).
[22] F. Bertazzi, M. Goano, and E. Bellotti, Appl. Phys. Lett. **101**, 011111 (2012).
[23] The vacuum level is 2.3 eV above the Fermi level. The high energy threshold is 2 eV above the vacuum level at low injected current (see structure diagram), that is 4.3 eV above the Fermi level. If we assume that the Fermi level is 0.2 eV above the bulk p-type GaN valence band, the minimum of the p-type GaN CB in the bulk is 3.2 eV above the Fermi level. The high energy threshold is thus $4.3 - 3.2 = 1.1$ eV above the minimum of the CB in the bulk p-GaN.
[24] F. Gütle *et al.*, Semicond. Sci. Technol. **27**, 125003 (2012).
[25] S. Wu, P. Geiser, J. Jun, J. Karpinski, D. Wang, and R. Sobolewskia, J. Appl. Phys. **101**, 043701 (2007).
[26] Ohmic potential drop in the p-type GaN region would not produce an energy shift of the Auger peak (electrons in the L valley will follow the progressive potential drop across the p-type GaN thickness). Ohmic potential drop at the p contact is already taken into account and produces a shift of the low energy edge. The only possibility for shifting the Auger peak is thus a rectification at the metal–p-type GaN contact.
[27] J. L. Shaw, R. E. Treece, D. Patel, C. S. Menoni, J. R. Smith, and J. I. Pankove, Appl. Phys. Lett. **81**, 3076 (2002).